Rubidium Impurity Diffusion in a Poly(ethylene oxide)−Sodium Iodide Polymer Electrolyte

Shahmahmood Obeidi and Nicolaas A. Stolwijk*

Institut für Materialphysik and Sonderforschungsbereich 458, University of Münster, Wilhelm-Klemm-Strasse 10, D-48149 Münster, Germany

Received: June 30, 2006; In Final Form: August 29, 2006

Diffusion of the radioisotope ^{86}Rb in an amorphous polymer−salt complex consisting of poly(ethylene oxide) and sodium iodide was found to be faster at all temperatures investigated than tracer self-diffusion of the smaller alkali metal cation ^{22}Na. This is the striking result of the first study on impurity diffusion in a polymer electrolyte system and a comparison with ionic self-diffusion and conductivity data previously obtained from the same system. The experimental findings can be rationalized within an ion transport model based on the occurrence of charged single ions and neutral ion pairs. Simultaneous analysis of all data revealed that the diffusivity of Rb^+ is likely to be lower than that of Na^+. Similarly, the diffusivity of RbI^0 pairs was found to be smaller than that of NaI^0 pairs. Surprisingly, the faster overall transport of Rb as measured by radiotracer diffusion appears to be due to a relatively large fraction of RbI pairs, in conjunction with the finding that the ion pair diffusivities exceed the single cation diffusivities by 2 orders of magnitude.

1. Introduction

Complexing suitable polymers with alkali metal salts may lead to ion-conducting materials with a combination of properties that are useful for application in rechargeable lightweight batteries. However, the ion migration mechanisms in these polymer electrolytes are still poorly understood. Over the past decades, the majority of studies dealing with ionic transport were based on measurements of the electrical conductivity. Specifically, the dc conductivity comprises the joint contributions of cations and anions to the long-range transport of electrical charge. A method to determine the transport properties of cations and anions individually, particularly for liquidlike systems, is pulsed field gradient NMR.[1,2] Another method that allows for an ion-specific measurement of mass transport, that is, preferentially in highly viscous systems, is radiotracer diffusion.[3,4] Recent investigations on two different polyether−NaI electrolytes have shown that a combination of conductivity and radiotracer self-diffusion measurements provides quantitative information about the impact of ion-pair formation as a function of temperature.[5−7] In particular, it was found that cation transport is a comparatively slow process that mainly takes place through a small concentration of cation−anion pairs with a high mobility.

As far as is known, all studies on ionic transport in polymer electrolytes are concerned with the migration properties of the constituent ions. However, unlike conductivity and PFG-NMR analysis, radiotracer experiments offer the possibility of investigating not only ionic self-diffusion but also ionic impurity diffusion. This is due to the high sensitivity of nuclear radiation detection, which allows us to monitor concentrations of suitable radioisotopes in the parts per million range or below. In fact, impurity diffusion studies have considerably contributed to the basic understanding of atomic transport processes in metals and semiconductors.[8] This inspired us to explore the diffusion behavior of an ionic impurity tracer in a well-characterized amorphous polymer electrolyte host.

The chosen electrolyte, $PEO_{30}NaI$, consists of poly(ethylene oxide) (PEO) complexed with sodium iodide to an oxygen-to-Na ratio of 30. Ionic self-diffusion in this electrolyte was previously investigated over a wide temperature range with the aid of the radiotracers ^{22}Na and ^{125}I as well as by conductivity measurements. Rubidium was taken as a foreign ion since it is chemically related to Na and has a suitable radioactive isotope (^{86}Rb). Surprisingly, the results of this study show that the tracer diffusivity of Rb is higher than that of Na for all temperatures investigated, although Rb has a distinctly larger ionic radius. These seemingly contradictory facts can be reconciled, however, within an extension of the ionic transport model[5,9] earlier proposed to describe self-diffusion in polymer electrolytes. The simultaneous application of this (extended) model to the experimental data of all ionic species reveals the prominent role of cation−anion pairs. Specifically, we find that it is the relatively strong tendency toward RbI pair formation that makes the overall transport of Rb faster than that of Na.

2. Experimental Section

The materials, procedures, and methods used in this work are, in principle, the same as those described in our previous publications.[5,6] In this report, we only provide a brief survey of the main experimental features. Deviating and additional treatments are presented in more detail. To avoid contact with ambient moisture and air, all critical preparation steps and experimental procedures were carried out in closed containers or in a nitrogen-flushed glovebox.

For the Rb tracer diffusion experiments, a new batch of $PEO_{30}NaI$ material was prepared. To this aim, appropriate amounts of PEO with a molecular weight of 8×10^6 (98.4%,[10] Aldrich) and NaI (99%, Grüssing) were dried under dynamic vacuum at elevated temperature and subsequently dissolved in water-free acetonitrile. After evaporation of the solvent under dynamic vacuum, the newly synthesized material was characterized by differential scanning calorimetry (DSC) and Archimedes-type mass density measurements. After the first heating/cooling cycle, the only feature in the DSC thermographs was the endothermic peak near 67 °C due to the melting of PEO. The density of the new $PEO_{30}NaI$ batch was found to be

* Corresponding author. E-mail: stolwij@uni-muenster.de.

10.1021/jp064105l CCC: $33.50
Published on Web 10/12/2006

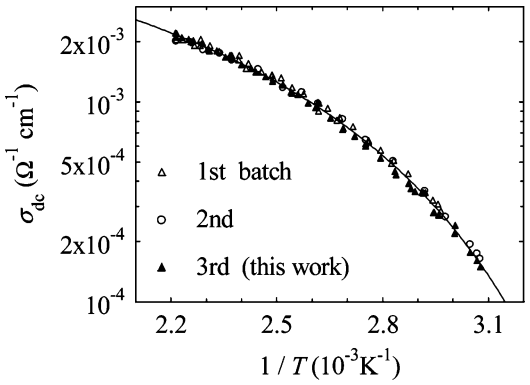

Figure 1. Direct current conductivity σ_{dc} of $PEO_{30}NaI$ as a function of inverse temperature. The data originate from three separately synthesized batches of sample material, as indicated (first batch,[5,6] second batch,[9] and third batch (this work)). The solid line is a fit of the VTF function to all data and is characterized by the following parameters: $B_\sigma = 329$ K, $T_{\sigma 0} = 248$ K, and $\sigma_0 = 0.011$ S cm^{-1}.

1.28 ± 0.02 g/cm^3, which agrees within experimental error with the earlier value of 1.26 ± 0.02 g/cm^3.[6]

Another test of the $PEO_{30}NaI$ batch properties and their reproducibility with respect to previous batches was performed by monitoring the dc conductivity σ_{dc} as a function of temperature. This was achieved by means of ac impedance spectroscopy in the frequency range of 5 Hz to 13 MHz during multiple heating and cooling cycles. To this aim, a cylindrical sample was held between stainless steel electrodes inside a temperature-controlled and nitrogen-flushed measuring cell. The thickness of the sample was determined from its mass by taking into account the mass density and the fixed surface area of the electrodes (1.00 cm^2). The result thus obtained was checked by directly measuring the thickness of the demounted sample after the last cooling cycle.

Figure 1 shows that the σ_{dc} values of the new $PEO_{30}NaI$ batch are close to those of the two previous batches[6,9] over the entire temperature range. The small differences of about 10% on the average are within the overall experimental error. This is taken as evidence that the three substances do not significantly differ in their chemical and physical properties.

The radioisotope ^{86}Rb with a half-life of 18.6 d was purchased from Perkin-Elmer in the form of an aqueous ^{86}RbI solution. Small amounts of this solution were dried under an infrared lamp, and then the residual radioactive salt was dissolved in acetonitrile. After the addition of some gellike $PEO_{30}NaI$ (containing acetonitrile) and subsequent stirring, the solution was cast on an inert support. Prolonged evaporation led to solvent-free $PEO_{30}NaI$ films of typically 40 μm thickness containing ^{86}Rb. Pieces of suitable size were cut from the radioactive film to serve as a diffusion source for hot-pressed cylindrical samples contained in suitable molds. In all cases, the Rb/Na concentration ratio of the source film was estimated to be smaller than 10^{-2}.

The diffusion treatment was performed in an oil bath at temperatures between 67 and 180 °C for time intervals between 6.5 and 0.5 h. At the end of the diffusion anneal, the encapsulated sample was quenched in water and subsequently sectioned at a temperature of about −50 °C using a rotary microtome. The β-activity of the sections was detected with the aid of a liquid scintillation counter.

3. Results

Figure 2 shows two typical ^{86}Rb diffusion profiles: one for the lowest temperature investigated, and the other for the highest.

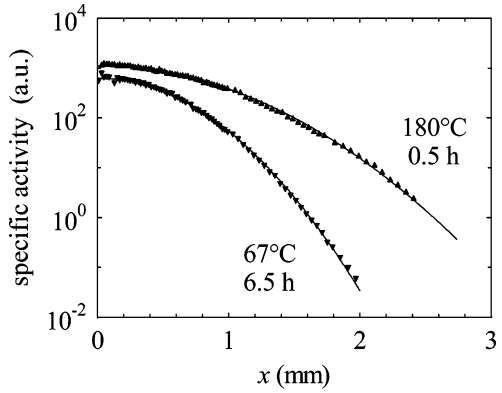

Figure 2. Depth profiles of ^{86}Rb in $PEO_{30}NaI$ resulting from different diffusion treatments, as indicated. The solid lines are best fits of the Gaussian function.

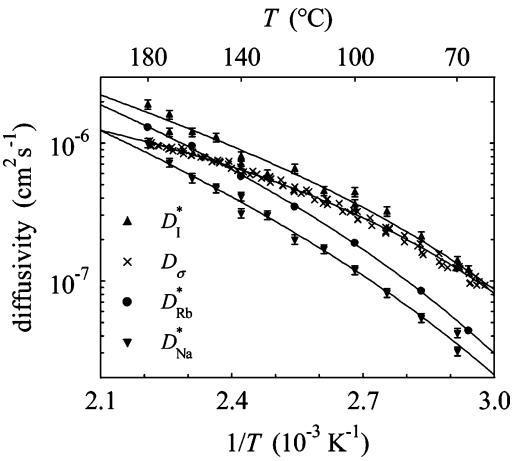

Figure 3. Tracer diffusion coefficient D^*_{Rb} of Rb in $PEO_{30}NaI$ (circles) compared to the tracer diffusivity of D^*_{Na} (▼) and D^*_I (▲), and to the charge diffusivity D_σ (×). The solid lines result from a simultaneous fit to all experimental data based on the ion migration model described in the text.

These profiles are fitted by the Gaussian function $c(x, t) = c(0, t)\exp(-x^2/4D^*t)$ (solid lines), where x denotes penetration depth, t is diffusion time, D is diffusion coefficient, and c is concentration (in arbitrary radioactivity units). The prefactor $c(0, t)$ is the actual concentration at $x = 0$. Also all other ^{86}Rb profiles unambiguously exhibit Gaussian shapes. This type of profile is representative of a constant diffusivity D^* (obtained by fitting) and instantaneous source conditions. Consequently, diffusion is accompanied by a deep exhaustion of the Rb source, so that, even near zero penetration depth, the Rb/Na ratio decreases to below 10^{-3}. Thus, the measured ^{86}Rb profiles are representative of impurity diffusion. In this case, chemical effects on the diffusion process may be neglected.

The ^{86}Rb diffusion coefficients D^*_{Rb} extracted from profile fitting are displayed in Figure 3 as a function of inverse temperature. Corresponding D^*_{Na} and D^*_I data from the diffusion of ^{22}Na and ^{125}I in $PEO_{30}NaI$[5,6] are also shown in Figure 3. The solid lines are least-squares fits resulting from the application of the migration model to be presented below.

Compared to D^*_{Na} and D^*_I, the D^*_{Rb} data show very little scatter, which manifests the improvement of some experimental skills with respect to the early measurements.[5,6] As a consequence, the curvature of D^*_{Rb} in the Arrhenius plot of Figure 2 can be easily recognized. This behavior, which is typical for transport processes in viscous systems, may be described by the Vogel−Tamman−Fulcher (VTF) equation given by $D^*_{Rb} =$

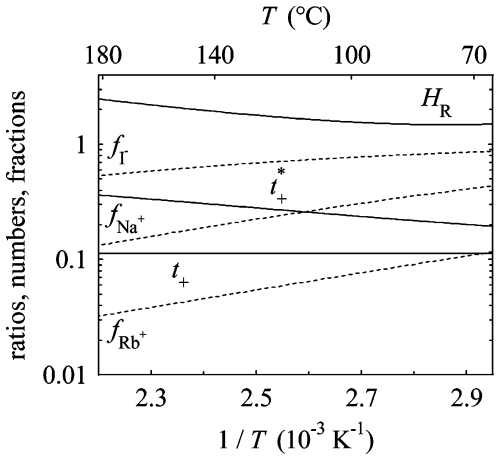

Figure 4. Temperature dependence of the Haven ratio H_R, the transport number t_+^*, and the transference number t_+ (solid lines). Additionally, the fractional diffusivity components f_{Rb^+}, f_{Na^+}, and f_{I^-} are plotted as dashed lines.

$D_{0,Rb}\exp[-B_{Rb}/(T - T_{0,Rb})]$. Adjusting this function to the D_{Rb}^* data yields $B_{Rb} = 1137$ K, $T_{0,Rb} = 194$ K, and $D_{0,Rb} = 1.06 \times 10^{-4}$ cm^2 s^{-1}. At this preliminary stage of analysis, no deeper meaning should be attributed to these parameter values; they just serve as a standard reference for comparison with other data.

It can be seen in Figure 3 that the tracer diffusion coefficients are ordered in magnitude according to $D_{Na}^* < D_{Rb}^* < D_I^*$ over the whole temperature range under consideration. In addition, the temperature dependence of D_{Rb}^* runs nearly parallel to that of D_{Na}^*. A comparison with the ionic impurity data in the literature is not possible since, to our knowledge, such data are not available.

Figure 3 also exhibits the temperature dependence of the charge diffusivity D_σ. These data were deduced from the σ_{dc} data shown in Figure 1 by using the Nernst−Einstein equation:

$$D_\sigma \equiv \frac{\sigma_{dc} k_B T}{C_s e^2} \tag{1}$$

where k_B denotes the Boltzmann constant, T is the temperature, and e is elementary charge. Taking the salt concentration C_s (i.e., number density) in the denominator of eq 3 implies that D_σ stands for the charge diffusivity per salt molecule; that is, D_σ comprises the joint effect of one cation and one anion.

Two quantities commonly used to characterize ionic transport in electrolytes can be directly calculated from the experimental data (smoothed by the VTF equation). The cation transport number $t_+^* = D_{Na}^*/(D_{Na}^* + D_I^*)$ expresses the relative contribution of cations to the total tracer diffusivity. The Haven ratio $H_R = (D_{Na}^* + D_I^*)/D_\sigma$ is a measure of the relative magnitude of the total tracer diffusivity with respect to the charge diffusivity.[11] Both quantities are displayed in Figure 4 together with other quantities to be introduced in section 6.2.

It is seen that t_+^* is much smaller than 1 for all temperatures under consideration. To be specific, t_+^* varies from 0.36 at 180 °C to 0.20 at 70 °C. These small cation transport numbers are at the low end of the range of similar data reported in the literature for a variety of polyether-based electrolytes.[4] However, a distinction must be made between the transport number t_+^* and the corresponding transference number t_+, which is based on the diffusivity of positive and negative charge carriers. It will be shown in section 6.2 that t_+ is even distinctly lower than t_+^*.

Figure 4 further shows that H_R assumes values greater than unity over the entire temperature range investigated. This differs from the situation in ionic conductors with one mobile charged species such as, for example, alkali metal oxide glasses, in which $H_R \leq 1$ generally holds.[12] However, Haven ratios greater than unity have been found in crystalline alkali halide systems where neutral vacancy pairs contribute to tracer diffusion but not to the ionic conductivity.[13]

A plausible reason for $H_R > 1$ in polymer electrolytes is the occurrence of cation−anion pairs, which contribute to mass transport ($D_{Na}^* + D_I^*$) but not to charge transport (D_σ).[14] Therefore, we attribute a major role to these electrically neutral ion pairs in the interpretation of our experimental data.

4. Modeling of Ionic Association and Diffusion

In previous reports on self-diffusion in $PEO_{30}NaI$,[5,6,9] we introduced the formation of NaI^0 pairs in terms of a chemical reaction between the ionized single species Na^+ and I^-. In this work, the in-diffusion of the foreign cation Rb led us to consider the possible formation of RbI^0 pairs due to the reaction:

$$Rb^+ + I^- \rightleftharpoons RbI^0 \tag{2}$$

Application of the mass action law to this reaction assumes the random mixing of all species and, moreover, sufficiently fast association and dissociation rates. Some evidence for the validity of these assumptions is given by the measured diffusion profiles, which unambiguously exhibit a Gaussian shape over 3 to 4 decades in concentration[15] (see Figure 2). Neglecting deviations from nonideality, e.g., due to electrostatic interactions,[16] we obtain

$$C_q = k'_q C_{Rb^+} C_{I^-} \tag{3}$$

This mass action equation relates the pair concentration C_q to the single-ion concentrations C_{Rb^+} and C_{I^-} through the ("true") reaction constant k'_q. Neglecting higher-order clusters, the total Rb concentration C_t equals $C_{Rb^+} + C_q$. Using similar mass conservation relations for Na and I,[5,9] we find from eq 2 an expression for the RbI^0 pair fraction r_q, viz.,[17]

$$r_q \equiv \frac{C_q}{C_t} = \frac{1}{1 + 1/[k_q(1 - r_p)]} \tag{4}$$

Here, $r_p \equiv C_p/C_s$ denotes the NaI^0 pair fraction, while $k_q \equiv k'_q C_s$ is introduced as a reduced reaction constant. The latter quantity may be decomposed into

$$k_q = k_{q0}\exp(-\Delta H_q/k_B T) \tag{5}$$

where ΔH_q represents the RbI^0 pair formation enthalpy, while the dimensionless prefactor k_{q0} equals $k'_{q0}C_s$. This expression is similar to the one previously introduced for the (reduced) NaI^0 pairing reaction constant $k_p = k_{p0}\exp(-\Delta H_p/k_B T)$ with the prefactor k_{p0} and the NaI^0 pair formation enthalpy ΔH_p.[5,9]

Given values of ΔH_q and k_{q0} enable us to calculate k_q with the aid of eq 5. Similarly, ΔH_p and k_{p0} determine k_p, which in turn allows for the calculation of r_p via the relationship $r_p = 1 + (1 - \sqrt{1+4k_p})/2k_p$.[5,9] Then r_q can be readily obtained using eq 4.

The tracer diffusion coefficient D_{Rb}^* comprises, in analogy to D_{Na}^*,[5,9] the joint effect of a charged cation contribution and a neutral pair contribution, according to

$$D_{Rb}^* = \hat{D}_{Rb^+} + \hat{D}_q \equiv (1 - r_q)D_{Rb^+} + r_q D_q \tag{6}$$

TABLE 1: Model Parameters and Their Statistical Error for $PEO_{30}NaI$[a]

B [K]	T_0 [K]	$D^0_{Na^+}$ [$cm^2\ s^{-1}$]	D^{-0}_{I} [$cm^2\ s^{-1}$]	D^0_p [$cm^2\ s^{-1}$]	k_{p0}	ΔH_p [eV]	D^{+0}_{Rb} [$cm^2\ s^{-1}$]	D^0_q [$cm^2\ s^{-1}$]	k_{q0}	ΔH_q [eV]
450	235	$9.7\cdot10^{-7}$	$7.6\cdot10^{-6}$	$8.0\cdot10^{-5}$	14	0.20	$8.3\cdot10^{-7}$	$6, 1\cdot10^{-5}$	24.1	0.19
±15%	±6%	±30%	±30%	±40%	±50%	±8%	±60%	±30%	±40%	±10%
464	234	$8.4\cdot10^{-7}$	$7.8\cdot10^{-6}$	$2.3\cdot10^{-4}$	2.1	0.17	$3.9\cdot10^{-7}$	$8.4\cdot10^{-5}$	8.5	0.16
±15%	±6%	±20%	±10%	±70%	±60%	±10%	±50%	±60%	±70%	±10%

[a] First row, left-side: from a simultaneous fit to all self-ion data (D^*_{Na}, D^*_I, and D_σ). First row, right side: from a separate fit to the Rb data (D^*_{Rb}). Second row: from a simultaneous fit to all self- and foreign-ion data (D^*_{Rb}, D^*_{Na}, D^*_I, and D_σ). For elucidation of the statistical error, see ref 23.

Here, D_{Rb^+} and D_q are the "true" diffusivities of Rb^+ and RbI^0, respectively. In contrast, their modifications $\hat{D}_{Rb^+}$ and $\hat{D}_q$, termed "effective" diffusion coefficients henceforward, make allowance for the relative abundance of the species of interest, that is, through the multiplication factors $(1 - r_q) = C_{Rb^+}/C_t$ and $r_q = C_q/C_t$.

For polymer electrolytes, there is reported evidence that the (true) diffusivity of any ionic or molecular species is intimately connected with the local motion of the polymer segments.[9,18,19] In the present context, this translates to (true) diffusivities all revealing the same VTF temperature dependence. Specifically, the two Rb-related diffusion coefficients take the following form:

$$D_{Rb^+} = D^0_{Rb^+} \exp[-B/(T - T_0)] \tag{7}$$

and

$$D_q = D^0_q \exp[-B/(T - T_0)] \tag{8}$$

In these expressions, B and T_0 are unique VTF parameters to be determined by data fitting (see below) and are usually referred to as the pseudo activation energy and the zero-mobility temperature, respectively. Similar expressions with the same B and T_0 values hold for D_{Na^+}, D_{I^-}, and D_p.[5,9] Nevertheless, the diffusivities will be different in magnitude because of the differences in the preexponential factor among and between foreign-ion related ($D^0_{Rb^+}$, D^0_q) and self-ion related ($D^0_{Na^+}$, $D^0_{I^-}$, D^0_p) species.

5. Data Fitting and Parameter Evaluation

In previous papers[5,9] dealing with $PEO_{30}NaI$, we simultaneously fitted the experimental data on tracer self-diffusivity and charge diffusivity by using the following set of equations:

$$D^*_{Na} = \hat{D}_{Na^+} + \hat{D}_p \equiv (1 - r_p)D_{Na^+} + r_p D_p \tag{9}$$

$$D^*_I = \hat{D}_{I^-} + \hat{D}_p \equiv (1 - r_p)\, D_{I^-} + r_p D_p \tag{10}$$

$$D_\sigma = \hat{D}_{Na^+} + \hat{D}_{I^-} = (1 - r_p)(D_{Na^+} + D_{I^-}) \tag{11}$$

Fitting involved the adjustment of seven free parameters, that is, B, T_0, $D^0_{Na^+}$, $D^0_{I^-}$, D^0_p, k_{p0}, and ΔH_p. The resulting best estimates of these parameters were taken from one of our earlier reports.[9,20] These data are compiled in the first row of Table 1 together with their statistical uncertainty.

In a first, simple approach to integrate the Rb tracer diffusivity in the existing transport model, the self-ion related parameter values included in Table 1 (first row) are considered to be fixed. As a consequence, only the Rb data have to be adjusted, that is, by the equation

$$D^*_{Rb} = [(1 - r_q)D^0_{Rb^+} + r_q D^0_q] \exp[-B/(T - T_0)] \tag{12}$$

which follows from eq 6 by using eqs 7 and 8. In this scenario, B and T_0 appear as known parameters in eq 12, while r_q includes the fixed values of k_{p0} and ΔH_p through its dependence on r_p (eq 4). Thus, only the remaining four parameters entering eq 12, that is, $D^0_{Rb^+}$, D^0_q, k_{q0}, and ΔH_q, need to be determined by fitting. The results are given in Table 1 (first row, right-hand side) along with the pertaining statistical tolerance.

The fit closely reproduces the experimental D^*_{Rb} data, as may be seen from the solid line in Figure 3 intersecting the solid circles.[21] Such a good fit had to be expected, since the number of adjustable parameters (i.e., four) is one more than that needed to obtain a VTF fit of similar quality. Apparently, this additional parameter is necessary to relieve the constraints imposed by the particular form of eq 12.[22] More important, however, is the finding that the pertinent parameter values appear to make physical sense, as elucidated next.

It can be inferred from Table 1 (first row) that the four Rb-related parameters are of closely similar magnitude relative to their (independently determined) Na-related counterparts. Specifically, $D^0_{Rb^+}$ and D^0_q are only 14% and 24% smaller than $D^0_{Na^+}$ and D^0_p, respectively. ΔH_q remains below ΔH_p by not more than 0.01 eV, whereas k_{q0} exceeds k_{p0} by less than a factor of 2.[23] All these differences are within the pertaining statistical uncertainties, also indicated in Table 1. However, the results of this simple analysis do not make allowance for possible variations in the self-ion parameters within their error ranges.

A second, more elaborate procedure to analyze the Rb tracer data involves the simultaneous fitting of all foreign- and self-ion diffusivities with the aid of eqs 6 and 9−11. This requires 11 free parameters, including two parameters (B, T_0) describing the common temperature dependence of all diffusion coefficients, five parameters ($D^0_{Na^+}$, $D^0_{Rb^+}$, $D^0_{I^-}$, D^0_p, D^0_q) determining the magnitude of the diffusivities, and four parameters (k_{p0}, ΔH_p, k_{q0}, ΔH_q) controlling the formation of NaI^0 and RbI^0 pairs, respectively. The best fit is represented in Figure 3 by the four solid lines covering the different sets of experimental data and characterized by the parameter values compiled in the second row of Table 1.

It is seen in Table 1 that the parameter values arising from the two different procedures of analysis compare well with each other. For most parameters, the difference between the first and second row values is not significant. Naturally, the changes in preexponential factors tend to be stronger than those observed for the other parameters.[23] The greatest disparity is found for k_p, which becomes lower by a factor 7. It should be emphasized that this change in k_p and the other six self-ion parameters is due to the inclusion of the Rb data and an additional (third) set of D_σ data in a simultaneous fitting procedure.

The physical picture connected with these parameter values (second row in Table 1) is illustrated by the Arrhenius plots of the true diffusion coefficients and the pair fractions in Figures 5 and 6, respectively. Figure 5 reveals the uniform temperature dependence of all diffusivities, as characterized by B and T_0. At the low end of the depicted diffusivity range, D_{Rb^+} is smaller

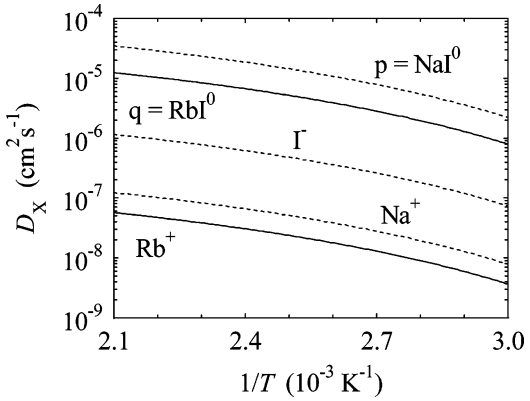

Figure 5. True diffusivity D_X of Rb-related (solid lines) and self-ion related (dashed lines) species X in $PEO_{30}NaI$ as a function of inverse temperature. X = p and X = q indicate NaI^0 and RbI^0 pairs, respectively.

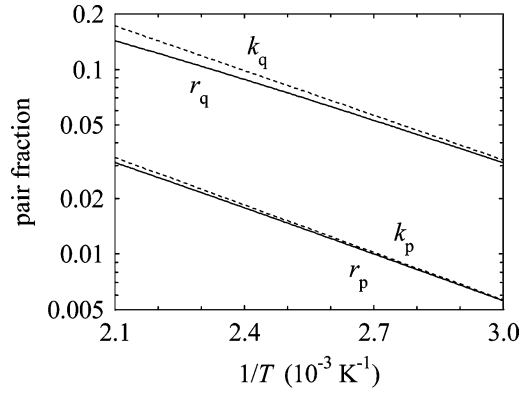

Figure 6. Fractions of RbI^0 (r_q) and NaI^0 (r_p) pairs (solid lines) and the associated (reduced) reaction constants (k_q, k_p; dashed lines) as a function of inverse temperature.

than D_{Na^+} by roughly a factor of 2. Similarly, at the high end of the same range, the diffusivity D_q of RbI^0 pairs remains below the diffusivity D_p of NaI^0 pairs by almost a factor of 3. In addition, D_{I^-} takes an intermediate position between the two low cation diffusivities and the two high pair diffusivities.

Figure 6 shows the pair fractions and the reduced reaction constants as a function of reciprocal temperature. The dashed lines representing k_q and k_p are nearly parallel, which reflects the finding that the pair formation enthalpies $\Delta H_q = 0.16$ and $\Delta H_p = 0.17$ (Table 1) are almost equal. Hence, our result that k_q exceeds k_p by about a factor of 5.5 is almost entirely due to the factor of 4 difference between the prefactors k_{q0} and k_{p0}. A similar difference in magnitude appears for the pair fractions r_q and r_p, as displayed by the solid curves in Figure 6. However, in going from low to high temperatures, the difference between r_q and r_p gradually becomes smaller, which is a consequence of the mass action law.

6. Discussion

6.1. Validity and Interpretation of the Parameter Results. In simultaneously fitting both Rb and self-ion data, 11 model parameters were adjusted, which is a large number. It should be noted, however, that even one more parameter, thus 12 in total, would be needed to fit each experimental diffusion coefficient (D_{Rb^+}, D_{Na^+}, D_{I^-}, D_σ) individually, for example, by the three-parameter VTF function. To gain additional confidence in the validity of our results, the fitting procedure was varied in different ways. First, instead of fitting $D^0_{Rb^+}$ and D^0_q in a straightforward manner (cf. Table 1), only their proportionality factors $D^0_{Rb^+}/D^0_{Na^+}$ and D^0_q/D^0_p with respect to the corresponding self-ion species were adjusted, yielding 0.42 (uncertainty of 60%) and 0.30 (60%), respectively.[23] This confirms the above result (Table 1, Figure 5) that the Rb-related species tend to move slower than the Na-related ones.

Furthermore, in an effort to reduce the number of free parameters, ΔH_q was set equal to ΔH_p. This resulted in a common pair formation enthalpy of 0.17 eV, close to the earlier individual values (Table 1), and a k_{q0}/k_{p0} ratio of 8.0 (50%), exceeding the former value by a factor of 2 (Figure 6). A further reduction to nine free parameters was achieved by additionally setting $D^0_{Rb^+} = D^0_{Na^+}$, which yielded 8.1×10^{-7} cm^2 s^{-1} for this common cation diffusivity and 0.17 eV (as before) for the common pair formation enthalpy. A close reproduction of the experimental data was also obtained by a 10 parameter fit due to setting D_q equal to D_p. This resulted in a common pair diffusivity of 1.8×10^{-4} cm^2 s^{-1}, which is intermediate with regard to the separate values in Table 1.

In all of the different fitting runs, the overall error statistics were comparably good, and the parameter values only changed within their uncertainty ranges indicated in Table 1. This confirms the physical picture of Rb impurity diffusion and self-diffusion in $PEO_{30}NaI$, which is represented by Figures 5 and 6 and characterized by the following features:

(i) Pairing of cations with anions plays a major role. This is true both for the constituent cations of the electrolyte (Na) and for the impurity cations (Rb). For Rb, the pair fraction is even higher than that for Na, that is, by about a factor of 5 for all temperatures of interest. This disparity appears to rely on differences in the preexponential factors of the pairing reaction constants (k_{q0}, k_{p0}), as the pair formation energies of RbI^0 and NaI^0 are closely similar. Therefore, it is the pair formation entropy that controls the relative pair abundance.

(ii) The ion pairs are much more mobile than the single cations. This may be due, on one hand, to the strong binding of Rb^+ and Na^+ to the ether oxygens of the polymer chains, and, on the other hand, to the weak interaction of the electrically neutral molecules RbI^0 and NaI^0 with the polymer matrix. The intermediate mobility of the anions may be explained by their rather indirect coupling to the polymer, i.e., via Coulombic forces between I^- and Na^+ (or Rb^+).

(iii) The true diffusivity of Rb^+ tends to be smaller than that of D_{Na^+}. Similarly, the RbI^0 pair is likely to move slower than the NaI^0 pair. This may be related to the fact that Rb has a larger ionic radius (152 pm) than Na (99 pm).

The notion that entropy plays a crucial role in pair formation is in accordance with other results. From the viewpoint of enthalpy, the pair state is not the favored one, since ΔH_p and ΔH_q are positive. Taking the values found for $k_{p0} = \exp(\Delta S_p/k_B)$ and $k_{q0} = \exp(\Delta S_q/k_B)$, the pair formation entropies ΔS_p and ΔS_q are also positive. Thus, the increase in the pair fractions with increasing temperature (Figure 6) is related to the growing importance of the entropy term in the Gibbs' free energy of pair formation. It seems natural to assume that a major entropy contribution results from the higher conformational freedom of the polymer upon the release of cations due to pair formation.[24−26]

Our finding that k_{q0} is significantly larger than k_{p0} suggests that Rb^+ becomes coordinated by more ether oxygens than Na^+. Hence, RbI^0 formation leads to the release of longer polymer segments than NaI^0 formation. This is consistent with the distinctly larger ionic radius of Rb compared to Na. In contrast to the pair formation entropies, the corresponding enthalpies ΔH_q and ΔH_p are very similar in magnitude. This indicates that the main factor in determining the pair formation enthalpy is the charge of the cation. The interaction of a "big" monovalent

cation with many oxygen atoms may be almost equivalent, in terms of overall enthalpy, to the interaction of a "small" monovalent cation with few oxygen atoms. Concomitantly, the enthalpy per cation−oxygen bond decreases with an increasing number of coordinating ether oxygens.

6.2. Effective Contributions to Charge and Mass Transport. The individual contributions of each mobile species to charge and mass transport can conveniently be evaluated in terms of effective diffusivities $\hat{D}_X = C_X D_X / C_s$ with $X = Rb^+$, Na^+, I^-, p, or q. (see eqs 6 and 9−11). The transference number t_+ measures the relative contribution of cations to the charge diffusivity according to

$$t_+ \equiv \frac{\hat{D}_{Na^+}}{D_\sigma} = \frac{\hat{D}_{Na^+}}{\hat{D}_{Na^+} + \hat{D}_{I^-}} = \frac{D^0_{Na^+}}{D^0_{Na^+} + D^0_{I^-}} \qquad (13)$$

In this expression, possible contributions or effects due to Rb may be neglected, since Rb diffusion takes place at very dilute concentrations. Thus, within the present model, t_+ is a temperature-independent quantity that obtains a value as low as 0.11 for $PEO_{30}NaI$. Figure 4 illustrates that t_+ is clearly smaller than the transport number t^*_+, which expresses the relative contribution of cations to the overall ionic mass transport (section 3). The reason for the difference between the transport and transference numbers lies in the occurrence of NaI^0 pairs, which affects t^*_+ but not t_+. Specifically, the increase in the pair fraction with increasing temperature is accompanied by an increase in t^*_+.

The Rb tracer diffusivity D^*_{Rb} comprises a single-ion and a pair component, as expressed by eqs 6 and 12. To quantify the relative contribution of Rb^+ to D^*_{Rb}, we introduce the fractional diffusivity component f_{Rb^+}, defined as

$$f_{Rb^+} \equiv \frac{\hat{D}_{Rb^+}}{D^*_{Rb}} = \frac{\hat{D}_{Rb^+}}{\hat{D}_{Rb^+} + \hat{D}_q} = \left(1 + \frac{r_q D^0_q}{(1 - r_q) D^0_{Rb^+}}\right)^{-1} \qquad (14)$$

Figure 4 shows f_{Rb^+} as a function of inverse temperature in comparison to $f_{Na^+} \equiv \hat{D}_{Na^+}/D^*_{Na}$ and $f_{I^-} \equiv \hat{D}_{I^-}/D^*_I$, which can be calculated by expressions similar to eq 14.[7]

It is seen in Figure 4 that f_{Rb^+} varies from 0.03 at the high end of the temperature range investigated (180 °C) to 0.11 at the low end (~70 °C). Consequently, Rb transport as measured by D^*_{Rb} takes place almost exclusively via RbI^0 pairs. For Na, the single-ion contribution is higher than that for Rb, as f_{Na^+} exceeds f_{Rb^+} at all temperatures. Nevertheless, the contribution of Na^+ to D^*_{Na} becomes substantial only at low temperatures. The highest fractional single-ion diffusivity is observed for the anion. Figure 4 shows that f_{I^-} increases from 0.52 to 0.87 with decreasing temperature, thus reflecting the lower importance of ion pairs for anion transport.

A comparison between the overall mass and charge transport is provided by the Haven ratio H_R, which, in the present context, is given by

$$H_R \equiv \frac{D^*_{Na} + D^*_I}{D_\sigma} = 1 + \frac{2\hat{D}_p}{\hat{D}_{Na^+} + \hat{D}_{I^-}} = 1 + \left(\frac{r_p}{1 - r_p}\right)\frac{2D^0_p}{D^0_{Na^+} + D^0_{I^-}} \qquad (15)$$

For $PEO_{30}NaI$, H_R adopts values roughly between 1.5 and 2.5, depending on temperature. This means that $\hat{D}_p$ is of similar magnitude to the mean effective diffusivity of single ions, denoted as $(\hat{D}_{Na^+} + \hat{D}_{I^-})/2$ (cf. the middle term in eq 15). The reference case is given by $H_R = 1$, which occurs when the effective diffusivity of neutral pairs can be neglected. Here, two limiting subcases should be distinguished. One applies to strong electrolytes in which there is virtually no pair formation ($r_p \approx 0$). The other extreme subcase is established when the existing ion pairs are practically immobile ($D_p \approx 0$). Thus, the observation that the Haven ratio is close to unity does not necessarily imply the absence of neutral pairs (or higher-order neutral clusters).

7. Conclusions

Our investigations on Rb diffusion in amorphous $PEO_{30}NaI$ by means of the radiotracer technique seem to represent the first study on ionic impurity diffusion in a salt-in-polymer electrolyte. The tracer diffusivity of Rb was compared not only with previously obtained tracer data of the self-ions Na and I, but also with the dc conductivity of the polymer−electrolyte substrate. The experimental results and their evaluation within an ion migration model based on charged single cations (Na^+, Rb^+), charged single anions (I^-), and neutral cation−anion pairs (NaI^0, RbI^0) led to the following conclusions: (i) The tracer diffusion coefficient of Rb is larger than that of Na for all temperatures investigated, although Rb is the "bigger" cation of the two. However, both cation tracers migrate slower than tracers of the anion (I). (ii) The true diffusivity (or mobility) of Rb^+ and RbI^0 tends to be lower than that of Na^+ and NaI^0, respectively, in agreement with a rule of thumb based on ionic or molecular size. However, the ion pairs are 2 orders of magnitude faster than the charged cations and 1 order of magnitude faster than the anions (I^-), which appears to anticorrelate with the strength of binding to the polymer chains. (iii) Rb exhibits a stronger tendency to form pairs than does Na. The resulting high pair fraction appears to be due to a larger pair formation entropy, whereas the pair formation enthalpies of Rb and Na are not significantly different. This relatively large entropy can be rationalized by the large ionic radius of Rb, which requires more ether oxygens and thus longer polymer segments for full cation coordination. (iv) The high tracer diffusivity of Rb with respect to Na follows from the higher Rb pair fraction in conjunction with the finding that the ion pairs move much faster than the charged single cations.

Acknowledgment. The authors gratefully acknowledge financial support by the Deutsche Forschungsgemeinschaft within the collaborative research center SFB 458.

References and Notes

(1) Boden, N.; Leng, S. A.; Ward, I. M. *Solid State Ionics* **1991**, *45*, 261.

(2) Arumugam, S.; Shi, J.; Tunstall, D. P.; Vincent, C. A. *J. Phys.: Condens. Matter* **1993**, *5*, 153.

(3) Chadwick, A. V.; Strange, J. H.; Worboys, M. R. *Solid State Ionics* **1983**, *9−10*, 1155. See also, Bridges, C.; Chadwick, A. V. *Solid State Ionics* **1988**, *28−30*, 965.

(4) Fauteux, D.; Lupien, M. D.; Robitaille, C. D. *J. Electrochem. Soc.* **1987**, *134*, 2761.

(5) Stolwijk, N. A.; Obeidi, Sh. *Phys. Rev. Lett.* **2004**, *93*, 125901.

(6) Obeidi, Sh.; Zazoum, B.; Stolwijk, N. A. *Solid State Ionics* **2004**, *173*, 77.

(7) Obeidi, Sh.; Stolwijk, N. A.; Pas, S. J. *Macromolecules* **2005**, *38*, 10750.

(8) Philibert, J. *Atom Movements−Diffusion and Mass Transport in Solids*; Les Éditions de Physique: Les Ulis, France, 1991

(9) Stolwijk, N. A.; Obeidi, Sh. *Diffus. Defect Data, Pt. A* **2005**, *237*, 1004.

(10) According to the pertaining lot specification, the base PEO material contained 1.4 wt % SiO_2 and 0.2 wt % CaO. These contaminations, which

are inherent to the manufacturing process, are present in the form of small particles. See also, Suarez, S.; Abbrent, S.; Greenbaum, S. G.; Shin, J. H.; Passerini, S. *Solid State Ionics* **2004**, *166*, 407.

(11) Lonergan, M. C.; Shriver, D. F.; Ratner, M. A. *Electrochim. Acta* **1995**, *40*, 2041.

(12) Voss, S.; Divinski, S.; Imre, A. W.; Mehrer, H.; Mundy, J. N. *Solid State Ionics* **2005**, *176*, 1383.

(13) Bonpunt, L.; Chanh, N. B.; Comberton, G.; Haget, Y.; Beniere, F. *Radiat. Eff.* **1983**, *75*, 33.

(14) Bruce, P. G.; Vincent, C. A. *Solid State Ionics* **1990**, *40*−*41*, 607.

(15) Stolwijk, N. A. *Phys. Rev. B* **1990**, *42*, 5793.

(16) Because of the high salt concentration (0.7 mol/kg) and the low dielectric constant (about 5) of $PEO_{30}NaI$, the consideration of electrostatic interactions must go beyond the application of (extended) Debye−Hückel theory. See, for instance, Pai, S. J.; Bae, Y. C.; Sun, Y. K. *J. Electrochem. Soc.* **2005**, *152*, A864. In this first report on impurity diffusion in a polymer electrolyte system, we refrain from such a complex analysis, also because the pertaining activity coefficients may only be slightly different from unity and rather weakly dependent on temperature.

(17) Equations 3 and 4 may be rewritten as $r_q = k_q(1 - r_q)(1 - r_p)$, which shows similarities to the mass action relationship for NaI^0 pair formation reading $r_p = k_p(1 - r_p)^2$.

(18) Furukawa, T.; Mukasa, Y.; Suzuki, T. Kano, K *J. Polym. Sci., Part B* **2002**, *40*, 613.

(19) Dürr, O.; Dieterich, W.; Nitzan, A. J. *Chem. Phys.* **2004**, *121*, 12732.

(20) Making allowance for a second set of D_σ data (arising from the second batch of $PEO_{30}NaI$), the parameter values in ref 9 differ from those in previous publications.[5,6] However, the differences are not significant within the pertaining experimental errors and statistical uncertainties.

(21) In fact, the solid line reproducing D^*_{Rb} in Figure 3 represents not only the "simple" fit to the Rb data alone (based on eq 12) but also the more elaborate fit involving both self-ion and Rb data (based on eqs 9−12). The minor differences between the two fitting curves are not visible in Figure 3.

(22) With B and T_0 given, it is the factor in square brackets in eq 12 that is fitted by least-squares minimization. This factor contains the closely interrelated functions r_q and $1 - r_q$, which have opposite curvatures in an Arrhenius plot (cf. Figure 6).

(23) Preexponential factors, such as D_0, enter the fitting procedure in the form of $\exp(\ln D_0)$, which yields better error statistics. The resulting standard deviations s_D in $\ln D_0$ (absolute values) lead to uncertainty factors of $\exp(\pm s_D)$. The specification $D_0 \pm 100\%$ corresponds to uncertainty factors of 2 (high bound) and 1/2 (low bound).

(24) Ratner, M. A.; Nitzan, A. *Faraday Discuss. Chem. Soc.* **1989**, *88*, 19.

(25) Schantz, S. *J. Chem. Phys.* **1991**, *94*, 6296.

(26) Stolwijk, N. A.; Wiencierz, M.; Obeidi, Sh. *Faraday Discuss.* **2007**, *134*; doi: 10.1039/b602143n